-Technical Paper-

MECHANICAL CHARACTERISTICS OF RC BEAMS WITH CORRODED STIRRUPS OR MAIN REINFORCEMENTS

Visal ITH*1, Koji MATSUMOTO*2 and Junichiro NIWA*3

ABSTRACT

This paper discusses the result of an experimental program designed to investigate the shear behavior of RC beams with corroded stirrups or main reinforcements. In the loading test of stirrup corrosion beams, the image analysis was conducted, and the result indicated that the shear cracking load increased due to the opening and sliding along the vertical corrosion cracks induced by the stirrup corrosion. Even non-corroded stirrups were provided to the RC beams with main reinforcement corrosion, the formation of arch action was observed.

Keywords: shear capacity, stirrup corrosion, main reinforcement corrosion, corrosion cracks, shear cracking load, sliding, arch action

1. INTRODUCTION

Reinforced concrete (RC) structures are often exposed directly to the atmosphere subjected to natural drying and wetting cycles, carbonation and chloride attacks. Such structures are vulnerable to deterioration problems associated with the corrosion of steel reinforcements. Thus, the study on mechanical properties of RC beams with corroded reinforcements has been becoming significant, as the result, a number of studies had been reported. Pimanmas et al. [1] studied the shear behavior of RC beams having penetrating pre-cracks. The reversed flexural loading was applied to induce the vertical cracks to the RC beams without stirrups, before conducting the shear loading test. During the test, the propagation of diagonal cracks was stopped due to low traction transfer along vertical penetrating pre-cracks, resulted in the increase of shear capacity. In 2007, Yamamoto and Miyagawa [2] reported the experimental results of RC beams with stirrup corrosion induced by the electrolytic corrosion test. It was found that in case that mass reduction ratio of stirrups (corrosion degree) was under 10%, the shear capacity of beams was increased due to the presence of vertical cracks caused by stirrup corrosion. However, the increase of shear capacity had not been quantitatively and precisely evaluated.

Tsunoda et al. [3] and Mori et al. [4] studied the influence of main reinforcement corrosion of RC beams on shear failure mechanism. The electrolytic corrosion test was used to induce the corrosion to main reinforcements of RC beams without stirrup. The experimental results showed the increase of shear capacity due to the formation of arch action caused by main reinforcement corrosion. However, the formation of arch action has not been investigated yet, in case of RC beams with stirrups.

In this study, two series of specimens, which consisted of RC beams with stirrup corrosion and main reinforcement corrosion, were prepared. The corrosion acceleration test by dry-wet cycle, whose phenomenon is similar to natural drying and wetting cycles of environment, was used to induce the corrosion to reinforcements. In the loading tests of stirrup corrosion beams, the image analysis was conducted to capture the cracking behavior in detail. The objective of this study is to investigate the mechanical characteristics of RC beams with corroded stirrups or main reinforcements.

2. EXPERIMENTAL PROCEDURES

2.1 Outline of the Specimens

The geometrical shape, dimensions, and the arrangement of reinforcements of stirrup corrosion and main reinforcement corrosion beams are shown in Fig. 1 and 2, respectively. All specimens were designed to fail in the shear tension failure mode with the safety margin of shear strength around 0.7 for stirrup corrosion specimens, and around 0.5 to 0.6 for main reinforcement corrosion specimens, as shown in Table 1. The total length of a beam was 1500 mm, with rectangular section of 150 mm width and 200 mm height. For series 1, normal steel was used as stirrups to induce corrosion, while stainless steel was used as main reinforcements and compression steel bars to avoid the corrosion. Reversely, normal steel was used as main reinforcement, while stainless steel was used as stirrups and compression steel bars for the specimens in series 2. In each series, all specimens were the same design, but different stirrup corrosion degree for the specimens in series 1, and different corrosion crack width for the specimens in series 2. In addition, to avoid anchorage failure during the loading test of main reinforcement corrosion beams, epoxy resin was used to cover the

*1 Graduate Student, Dept. of Civil Engineering, Tokyo Institute of Technology, JCI Student Member
*2 Assistant Professor, Dept. of Civil Engineering, Tokyo Institute of Technology, Dr. E., JCI Member
*3 Professor, Dept. of Civil Engineering, Tokyo Institute of Technology, Dr. E., JCI Member

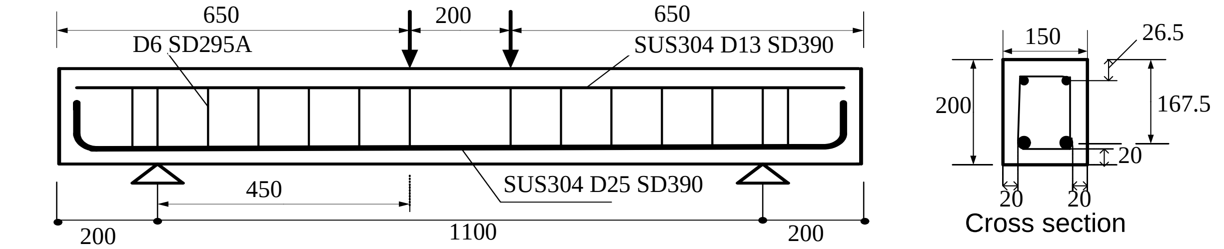

Fig. 1 Outline of stirrup corrosion specimen (Unit : mm)

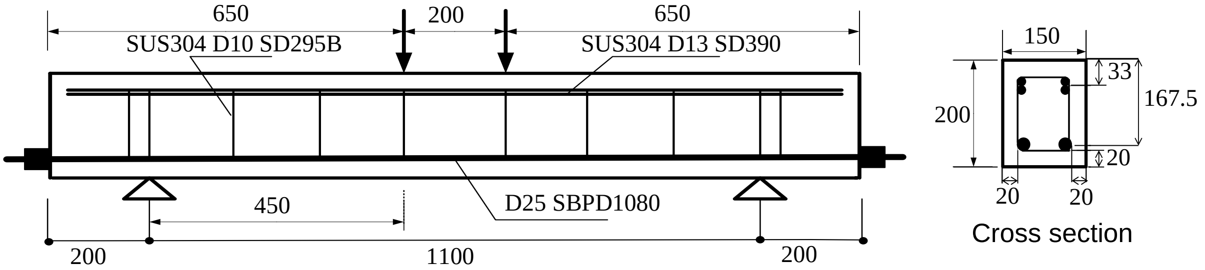

Fig. 2 Outline of main reinforcement corrosion specimen (Unit : mm)

Table 1 Calculated values of V_c, V_s, P_v and P_u

Specimens		Target corrosion degree (%)	Target corrosion crack width (mm)	f'_c (N/mm^2)	V_c (kN)	V_s (kN)	P_v (kN)	P_u (kN)	P_v/P_u
Series 1: Stirrup corrosion	SC00	0.00		49.3	58.3	33.0	182.6	251.1	0.727
	SC07	7.00		43.8	56.0	33.0*	178.0*	248.1	0.718
	SC13	13.0		45.8	56.8	33.0*	179.8*	249.6	0.720
Series 2 : Main rebar corrosion	MC00		0.00	45.6	56.8	51.6	216.8	360.1	0.602
	MC-cr0.25		0.25	50.8	58.8*	51.6	220.8*	382.5*	0.577
	MC-cr0.50		0.50	66.3	64.3*	51.6	231.8*	445.5*	0.520
	MC-cr1.00		1.00	52.2	59.4*	51.6	221.9*	388.4*	0.571

f'_c : compressive strength of concrete, V_c : shear carried by concrete, V_s : shear carried by stirrups
*: calculation in case no corrosion of reinforcement, P_v : shear failure load, P_u : flexural failure load

Table 2 Mix proportion of concrete

G_{max} (mm)	W/C (%)	s/a (%)	Unit weight (kg/m^3)					
			W	C	S	G	AE	$NaCl$
20	60	45	169.8	293.0	816.0	984.7	0.439	10.0

G_{max} : the maximum size of aggregate, s/a : sand percentage, W : water, C: cement, S: sand, G : coarse gravel, AE : water-reducing admixture


(a) Covered by epoxy resin (b) Fixed by nuts

Fig. 3 Anchorage zone

Table 3 Properties of reinforcement

Reinforcements		Type		Yield strength (N/mm^2)	Cross-section area (mm^2)
Series 1: Stirrup corrosion	Main reinforcement	Stainless steel	SUS304 D25 SD390	390	1013
	Compression steel	Stainless steel	SUS304 D13 SD390	410	253
	Stirrup	Normal steel	D6 SD295A	322	63
Series 2: Main rebar corrosion	Main reinforcement	High strength steel	D25 SBPD1080	1179	982
	Compression steel	Stainless steel	SUS304 D13 SD390	410	506
	Stirrup	Stainless steel	SUS304 D10 SD295A	369	143

main reinforcement in the anchorage zone to avoid corrosion, as shown in Fig. 3 (a). On the other hand, in order to prevent the beams from the anchorage failure during the loading test, the anchorage zone of beams was strengthened by FRP sheets, and fixed by nuts at both side of main reinforcements, as shown in Fig. 3 (b). The specimens SC00 and MC00 were the reference beams without any corrosion of reinforcement.

Table 2 shows the mix proportion of concrete. Ten kilogram of NaCl, which was equivalent to about 6.0 kg of Cl^- ion, was put into the mix proportion of the concrete for all specimens in this study. Table 3 shows the properties of the reinforcements.

2.2 Corrosion Acceleration Test

(1) Method to induce steel corrosion

The specimens were put into an environmental control chamber to accelerate the corrosion of reinforcements. During each cycle of dry-wet cyclic corrosion acceleration test, the temperature was set to 10 degree Celsius with 40% of relative humidity for 4 days of the dry period, and 60 degree Celsius with 95% of relative humidity for 3 days of the wet period.

(2) Investigation of corrosion level

After seven cycles of the dry-wet cyclic corrosion acceleration test, a number of vertical corrosion cracks appeared on the surface along the stirrups of the stirrup corrosion specimens. Crack width and the location of the cracks were recorded. As the corrosion degree (mass reduction ratio) of stirrups was the experimental parameter of the specimens in series 1, the investigation of corrosion degree of stirrups was needed to ensure whether the corrosion degree reached the target value.

In the experimental study conducted by Ikeda et al. [5], the electrolytic corrosion test was conducted to induce corrosion to main reinforcements, and it was concluded that the shear behavior of RC beams with main reinforcement corrosion is not directly related to the corrosion degree. It can be evaluated by the corrosion cracks because the bond of reinforcements, which affects the formation of arch action, is associated with the development of corrosion cracks. Therefore, the corrosion crack width was considered to be the experimental parameter for the specimens in series 2 in this study.

.

3. EXPERIMENTAL RESULTS

3.1 Result of Corrosion Acceleration Test

(1) Measurement of corrosion degree

After the loading test, all corroded reinforcements were taken out from the tested span of the RC beams. The weight loss of stirrups was measured by the following procedures. At first, corrosion products and concrete sticking to the surface of reinforcements were removed. Then, 24 pieces of 20 mm length (Fig. 4) of stirrups from tested span of corrosion specimens in series 1, and 11 pieces of 10 cm length of main reinforcement from corrosion specimens in series 2, was cut. Finally, those pieces of stirrups and main reinforcements were immersed in 10% diammonium hydrogen citrate solution with 60 degree Celsius for 2 days, to completely remove corrosion products.

To calculate the corrosion degree of reinforcements, the following equation was used.

$$R = \frac{(w_0 - w_c)}{w_0} \times 100 \qquad (1)$$

where, R is the corrosion degree (%), w_0 is the mass per unit length of original reinforcement (g/mm), w_c is the mass per unit length of corroded reinforcements after cleaning (g/mm). Figure 5 shows an example of the distribution of corrosion degree in each location of a stirrup. The lateral axis is corresponding to the numbers in Fig. 4. After measuring the corrosion degree of each stirrup in the shear span, small variation of corrosion degree was found. The average of corrosion degree of all stirrups in the shear span (r) was 6.55% and 13.2% for the specimen SC07, and SC13, respectively.

(2) Measurement of corrosion crack width of main reinforcement corrosion beams

Cracks along the main reinforcements were investigated on the bottom surface of main reinforcement corrosion specimens after eight cycles of dry-wet cycle test. No corrosion cracks appeared on the side surfaces of the specimens. Then, the surface crack width was measured in 10 cm interval to calculate the average corrosion crack width. After the loading test, the corrosion degree of main reinforcement was also measured. Difference from the corrosion accelerated by electric corrosion test in the previous study [3] and [4], the flow of corrosion products from the beams was not observed in the dry-wet cycle test. This difference

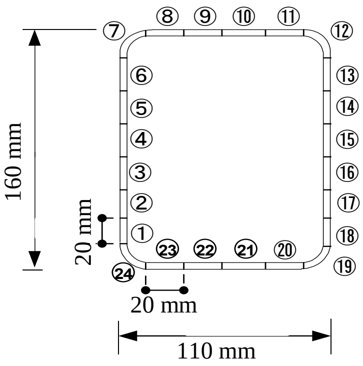

Fig. 4 Division of corroded stirrup

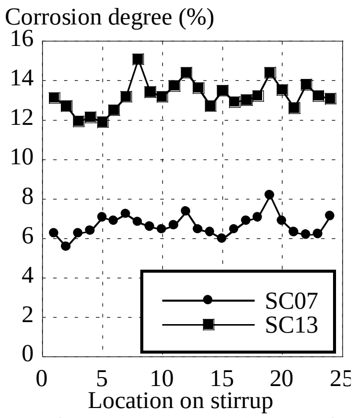

Fig. 5 Example of corrosion degree of stirrup

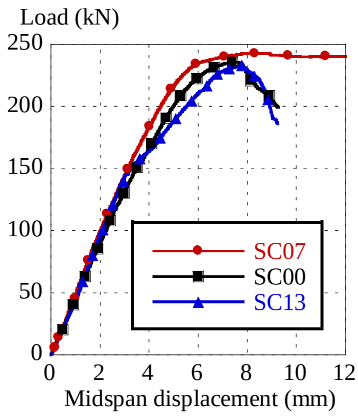

Fig. 6 Load-midspan displacement curve

Table 4 Results of acceleration corrosion test

Specimens		N	Target		Experimental results		Previous studies ([3] and [4])		
			This study					Experimental results	
			Cr (mm)	r (%)	Cr (mm)	r (%)		Cr (mm)	r (%)
Series 1: Stirrup corrosion	SC00	0		0.00	0.00	0.00			
	SC07	18		7.00	0.15	6.55			
	SC13	25		13.0	0.20	13.2			
Series 2: Main rebar corrosion	MC00	0	0.00		0.00	0.00			
	MC-cr0.25	16	0.25		0.25	4.27	[3]	0.27	7.8
	MC-cr0.50	22	0.50		0.44	5.17			
	MC-cr1.00	26	1.00		0.83	6.93	[4]	0.82	12.5

N : number of dry-wet cycle test, *Cr* : the average of corrosion crack width, *r* : the average of corrosion degree of corroded reinforcements in the shear span

can be considered as a reason that the dry-wet cycle test produced comparatively wider crack width with lower corrosion degree of main reinforcements (Table 4).

3.2 Result of loading test

(1) Stirrup corrosion specimens

a) Failure process

Figure 6 shows the relationship between load and midspan displacement. After the flexural crack happened at about 25 kN, a diagonal crack was seen in the reference beam SC00 at 85 kN. However, at the same load level, the diagonal crack could not be observed in the corrosion specimens, until the load reached 141 kN for the specimen SC07, and 155 kN for SC13 (Table 5). Finally, SC00 was failed in shear with the maximum load of 235 kN. The experimental value of shear capacity of the beam was increased higher than the calculated value shown in Table 1.

Moreover, even the compressive strength of concrete of SC07 was lower than that of SC00, the flexural failure occurred in SC07. It indicates that even there are 6.55% of stirrup corrosion, the shear capacity of SC07 was increased.

However, when the corrosion of stirrups increased to 13.2%, the failure mode of the beam changed to shear failure again. As shown in Table 5, the specimen SC13 failed in 231 kN, slightly lower than that of SC00.

b) Image analysis result

The image analysis was conducted to capture the corrosion cracks behavior in detail. Crack opening and sliding along the corrosion cracks induced by the stirrup corrosion were investigated. Here, the results at P = 115 kN which was almost equal to the calculated value of V_c, and P = 170 kN, at which diagonal cracks already occurred, were selected. Figure 7 shows the increase of corrosion crack width in tensile part of the beam (from the neutral axis to the bottom) at location R1, R2 and R3 as showed in Fig. 8. The neutral axis was about 120 mm from the bottom of the beams. In case of P = 115 kN, the crack opening at all locations under the neutral axis increases with the increase in bending moment, and provided the maximum value at the bottom of the beam. However, for specimen SC07 in case of P = 170 kN, at location R2 and R3, the crack width became the maximum at about 80 mm from the bottom of the beam (Fig. 7 (a)). It was because the shear stress, which became the maximum value at the middle depth of the beam, produced stronger tensile stress, affected the opening of crack width.

Moreover, the vertical cracks induced by the stirrup corrosion divided the shear span into blocks, as shown in Fig. 8. When the load is applied to a beam, sliding between two concrete blocks on both sides of vertical cracks happens. The amount of sliding was obtained overall the depth of the beam, as shown in Fig. 9. The value of sliding at location R2 was bigger than that of R3 due to the effect of bending moment. However, even the bending moment at location R1 was the biggest, the amount of sliding at this location was smaller than that of R2 and R3. This is because the vertical crack at location R1 was under the loading plate which covered both side of concrete blocks.

From the above results, it indicated that the opening and sliding along corrosion cracks could be considered as the reason that delayed the formation of diagonal crack in both SC07 and SC13. However, even the increase of shear cracking load was observed in SC13, the decrease of shear carried by stirrups due to about 13.2 % of stirrup corrosion dramatically influenced the shear capacity, resulted in the decrease of shear failure load. This result has also shown that, even vertical corrosion cracks exist, the tensile stress which generates the diagonal cracks still happened because of the effect of non-corroded main reinforcements.

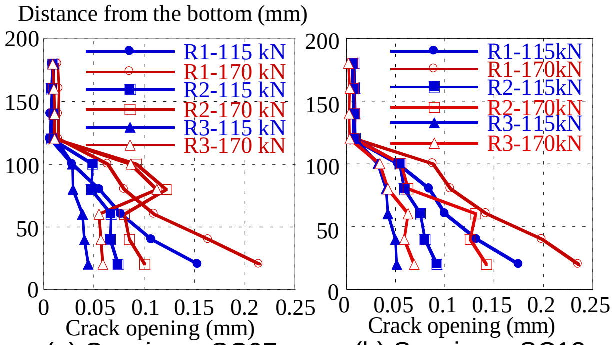

(a) Specimen SC07 (b) Specimen SC13

Fig. 7 Distribution of opening corrosion cracks

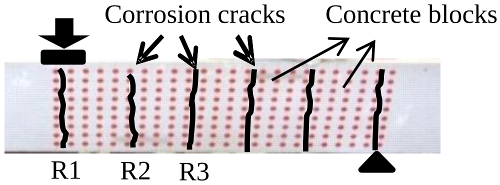

Fig. 8 Corrosion cracks (series 1)

Table 5 Results of loading test

Specimens	f'_c (N/mm^2)	f_t (N/mm^2)	E_c (N/mm^2)	Load at diagonal crack (kN)	P_{max} (kN)	Failure mode
SC00	49.3	3.88	28.6	85.0	235	Shear tension
SC07	43.8	3.12	26.9	141.0	242	Flexural
SC13	45.8	3.22	27.0	155.0	231	Shear tension
MC00	45.6	2.30	27.0	95.0	275	Shear tension
MC-cr0.25	50.8	2.40	28.9	121.0	306	Shear tension
MC-cr0.50	66.3	3.47	32.8	129.0	296	Shear tension
MC-cr1.00	52.2	2.66	29.6	132.0	322	Shear tension

f'_c: compressive strength of concrete, f_t: tensile strength of concrete, E_c: Young's modulus of concrete, P_{max} : maximum load

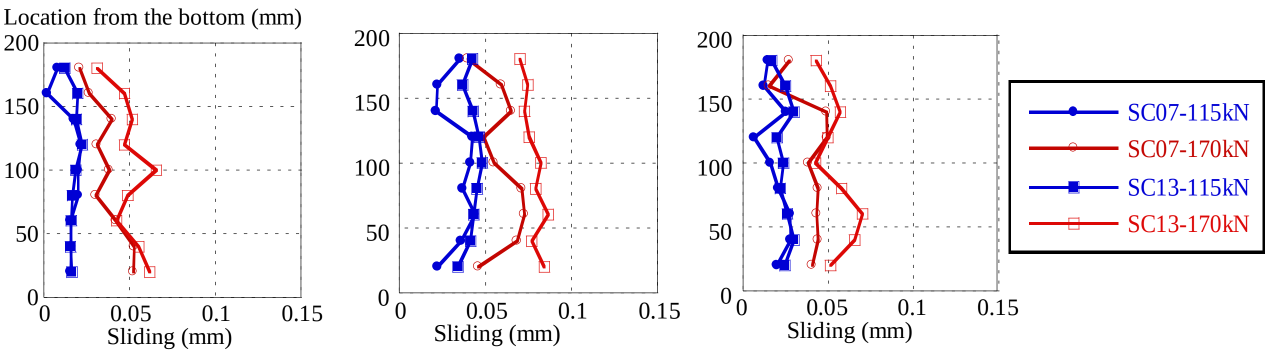

(a) Location R1 (b) Location R2 (c) Location R3

Fig. 9 Sliding along corrosion cracks

(2) Main reinforcement corrosion specimens

a) Failure process

Figure 10 shows the relationship between the load and midspan displacement of all beams in series 2. All specimens failed in shear. The crack pattern of the beams at the failure load is illustrated in Fig. 11.

For no corrosion beam MC00, first, bending cracks initially propagated around the span center, before the occurrence of a diagonal crack at 95 kN. After that, a single clear diagonal crack developed slowly by linking the loading point and the support, as shown in Fig. 11 (a). Finally, the width of the diagonal crack increased, and the increase in load became slow, and then, the beam failed in shear with the maximum load of 275 kN.

For the corrosion specimen MC-cr0.25, at first, a diagonal crack happened at 121 kN at the middle of shear span, and it slowly developed toward the support and loading point. However, this diagonal crack did not keep progressing up to the loading point, while another diagonal crack appeared in the upper part (Fig. 11 (b)) at 283 kN. Finally, the beam failed when the upper diagonal crack progressed until the loading point at 306 kN. This result represented the increase in the shear capacity about 11%, compared to the reference beam. The increase in shear capacity was the consequence of the formation of tied arch action due to the corrosion of main reinforcements.

The similar failure process was investigated in the specimen MC-cr1.00. As shown in Fig. 11 (d), two main shear cracks were observed. The shear capacity of the beam was 322 kN, representing the increase about 17%, compared to the reference beam. From the above results, it can be concluded that the shear capacity of RC beams with corroded main reinforcement increases with the increase in corrosion crack width along the main reinforcements.

However, the specimen MC-cr0.50 which consisted of about 0.44 mm of corrosion crack width, failed at a maximum load of 296 kN. It represented only about 8% increase in shear capacity, compared to the reference beam, indicating slight decrease in shear capacity compared to the specimen MC-cr0.25 (Table 5). In this case, as shown in Fig. 11 (c), the increase in inclination angle of the diagonal crack, which resulted in the decrease in shear carried by stirrups, can be considered as the reason. The average value of inclination angle of diagonal crack ($\theta_{mea.}$) shown in Table 6 was obtained by the following procedures. First, a straight line, which connected the top end of the diagonal crack to the intersecting point of diagonal crack with main reinforcement, was drawn. Then the angle between this line and the horizontal line was measured. This angle was considered to be the inclination angle of a diagonal crack. Finally, the angle was measured on both side surfaces of the failure shear span, and the average value was calculated.

b) The effect of stirrups

The increase in shear capacity due to arch action (V_{arch}) can be obtained from Eq. (1).

$$V_{arch} = V_{ex} - V_c - V_s \qquad (1)$$

where, V_{ex} is the shear capacity from the experiment, V_c is the calculated value of shear carried by concrete,

Table 6 Increasing amount of shear capacity due to arch action

Specimens	$\theta_{mea.}$ (degree)	V_c (kN)	V_s (kN)	V_{ex} (kN)	V_{arch} (kN)	V_{arch}/V_c (%)
MC00	34.3	56.8	80.8	137.5	0	0
MC-cr0.25	32.5	58.8*	75.7	153.0	18.5	31.5
MC-cr0.50	41.1	64.3*	65.5	148.0	24.6	38.3
MC-cr1.00	33.4	59.4*	78.3	161.0	23.3	39.2

$\theta_{mea.}$: measurement value of inclination angle of diagonal crack, V_c: shear carried by concrete, V_s: shear carried by stirrups, V_{ex}: shear capacity from the experiment, V_{arch} : increasing amount of shear capacity due to the formation of arch action. * : calculation in case of no corrosion of main reinforcement.

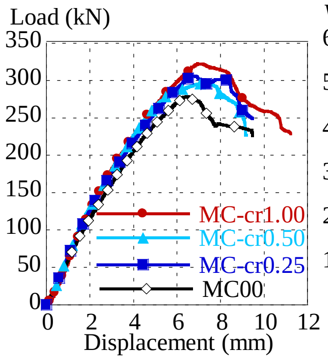

Fig. 10 Load-midspan displacement curve

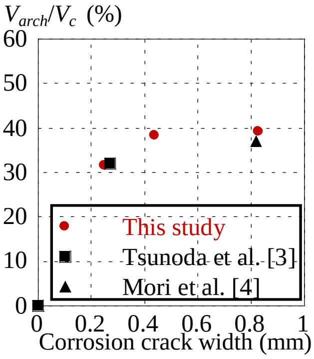

Fig. 12 Increasing ratio of shear capacity carried by arch action

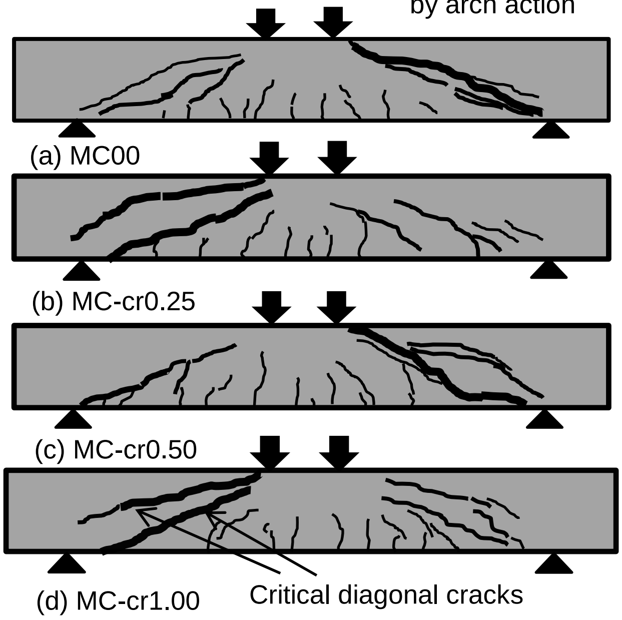

Fig. 11 Crack pattern at failure load of specimens in series 2

and V_s is the shear carried by stirrups. The increasing of shear capacity due to the formation of arch action (V_{arch}) , and the increasing ratio V_{arch}/V_c was shown in Table 6.

The comparison of the increasing ratio of shear carried by concrete due to the main reinforcement corrosion, in case RC beams with stirrups in this study and beam without stirrup conducted by [3] and [4], was illustrated in Fig. 12. The result indicates that arch action produced the same amount of increasing ratio in RC beams either with or without stirrups. Thus, it can be concluded that, the existing of stirrups has no effect on the increasing amount of shear capacity carried by arch action.

4. CONCLUSIONS

(1) The shear capacity of the RC beam with 6.55% of stirrup corrosion degree was increased. From the result of the image analysis, the reason is the increase in shear cracking load due to the opening and sliding along the vertical cracks induced by the stirrup corrosion. However, when the corrosion of stirrups increased to 13.2%, the shear capacity was slightly decreased. In this case, even the increase of shear cracking load was observed, the decrease of shear carried by stirrups due to stirrup corrosion was considered to affect the shear capacity, resulted in the decrease in failure load.

(2) Even non-corroded stirrups were provided to the beams with main reinforcement corrosion, the formation of arch action was observed. The formation of arch action resulted in the increase in shear capacity.

(3) The arch action produced the same amount of increasing ratio in RC beams either with or without stirrups. Thus, the presence of stirrups has no effect on the increasing amount of shear capacity carried by arch action.

REFERENCES

[1] Pimanmas, A., Hosoda, A. and Maekawa, K., "Shear behavior of RC beams containing vertical penetrating pre-cracks", JSCE conference, V-519, 2000, pp. 1040-1041.

[2] Yamamoto, T. and Miyagawa, T., "Mechanical performance of RC structural material and member deterioration by corrosion of reinforcing steel", Journal of the society of materials science, Vol. 56, No. 8, 2007, pp. 684-693. (in Japanese)

[3] Tsunoda, M.,Watanabe, K. and Niwa, J., "Shear behavior of RC beams with partial corrosion of main reinforcements.", Proceeding of JCI, Vol. 31, No. 2, 2009, pp. 1561-1566. (in Japanese)

[4] Mori, M., Matsumoto, K. and Niwa, J., "Mechanical properties of RC beams with corroded main reinforcement at anchorage part or shear span." Proceeding of JCI, Vol. 35, No. 2, 2013 pp. 547-552. (in Japanese)

[5] Ikeda, H., Murakami, Y., Oshita, H. and Tsutsumi, T., "Influence of reinforcement corrosion on shear resistance of RC beams", Proceeding of JCI, Vol. 31, No. 2, 2009, pp. 769-774. (in Japanese)